



Contents lists available at ScienceDirect

Bioorganic & Medicinal Chemistry Letters

journal homepage: www.elsevier.com/locate/bmcl

Potent antiprotozoal activity of a novel semi-synthetic berberine derivative

Mark Bahar^a, Ye Deng^a, Xiaohua Zhu^a, Shanshan He^a, Trupti Pandharkar^a, Mark E. Drew^{a,b}, Armando Navarro-Vázquez^c, Clemens Anklin^e, Roberto R. Gil^d, Raymond W. Doskotch^a, Karl A. Werbovetz^a, A. Douglas Kinghorn^{a,*}

^a College of Pharmacy, The Ohio State University, Columbus, Ohio 43210, USA^b College of Medicine, The Ohio State University, Columbus, Ohio 43210, USA^c Departamento de Química Orgánica, Universidade de Vigo, Vigo 36310, Spain^d Department of Chemistry, Carnegie Mellon University, Pittsburgh, PA 15213, USA^e Bruker BioSpin Corp., 15 Fortune Dr., Billerica, MA 01821, USA

ARTICLE INFO

Article history:

Received 10 December 2010

Revised 21 January 2011

Accepted 21 January 2011

Available online 27 January 2011

Keywords:

Berberine

5,6-Didehydro-8,8-diethyl-13-

oxodihydroberberine chloride

African trypanosomiasis

Leishmaniasis

Malaria

Inhibitory activity

ABSTRACT

Treatment of diseases such as African sleeping sickness and leishmaniasis often depends on relatively expensive or toxic drugs, and resistance to current chemotherapeutics is an issue in treating these diseases and malaria. In this study, a new semi-synthetic berberine analogue, 5,6-didehydro-8,8-diethyl-13-oxodihydroberberine chloride (**1**), showed nanomolar level potency against in vitro models of leishmaniasis, malaria, and trypanosomiasis as well as activity in an in vivo visceral leishmaniasis model. Since the synthetic starting material, berberine hemisulfate, is inexpensive, 8,8-dialkyl-substituted analogues of berberine may lead to a new class of affordable antiprotozoal compounds.

© 2011 Published by Elsevier Ltd.

Malaria, leishmaniasis, and human African trypanosomiasis are diseases caused by protozoan parasites that affect the poorest inhabitants of the world disproportionately and hinder the economic development of the afflicted societies significantly.^{1–3} The life cycles of the causative parasites are complex and the diseases are not easy to diagnose in the early stages when chemotherapeutic intervention is most effective. Also, social, economic and political factors do not always favor intervention efforts, and the drugs used currently for therapy may be either toxic, expensive, or difficult to use in the field. From a drug discovery perspective, efforts to find new effective drugs do not appear to match the toll these diseases take on the lives of the poorest global inhabitants, living mainly in Africa, Asia, and Latin America.^{4–9}

Berberine is a benzyl-tetrahydroisoquinoline-type quaternary alkaloid biosynthesized by species in the plant families Berberidaceae and Ranunculaceae, with certain of these plants having been long used in traditional medicine for various ailments.¹⁰ Berberine and its natural and semi-synthetic analogues have been studied extensively for their diverse anti-infective and other pharmacolog-

ical effects.^{11–15} Of particular interest, a number of berberine-type alkaloids have exhibited antiprotozoal activity in both in vitro and in vivo assay systems.^{16–22}

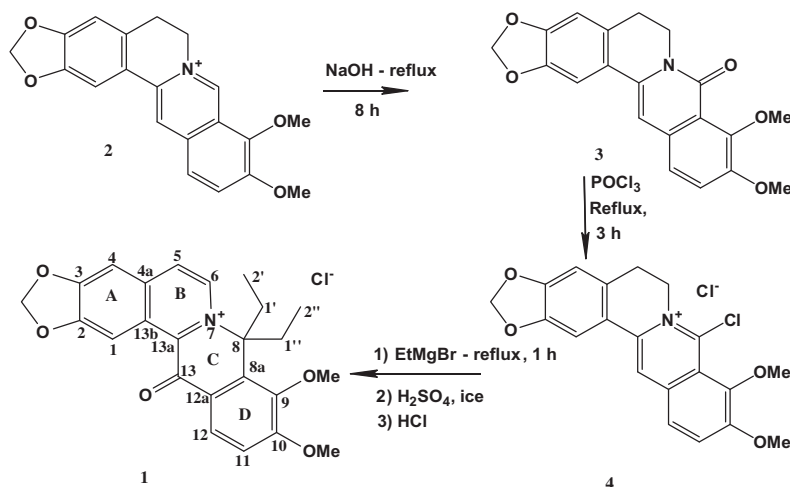
Herein, we describe the synthesis (Scheme 1), structure elucidation, and potent in vitro and in vivo activities of 5,6-didehydro-8,8-diethyl-13-oxodihydroberberine chloride (**1**), a previously unreported compound.

The use of 8-chloroberberine (**4**) as a means to produce various semi-synthetic analogues of berberine has been described previously.²³ While data are available regarding the bioactivity of 8-monosubstituted berberine derivatives,²⁴ 8-chloroberberine reacts readily with Grignard reagents, providing a viable synthetic route to dialkyl substitution at this position.^{23,25}

When the synthesis steps were carried according to a previous report²³ (Scheme 1), the major product turned out to be 5,6-didehydro-8,8-diethyl-13-oxodihydroberberine chloride (**1**, 0.9 mmol, 36% yield, see Supplementary data), a new semi-synthetic berberine derivative. This structure varies from the previously proposed structure at the positions C-13 where an oxidation had occurred and between the C-5 and C-6, where a double bond was formed through oxidation. While this finding was unexpected, similar modifications in the isoquinoline ring system have been reported previously^{23e} and are thought to result from the iminobenzylic anion by aerial oxidation. Accordingly,

* Corresponding author. Tel.: +1 614 247 8094; fax: +1 614 247 8642.

E-mail address: kinghorn@pharmacy.ohio-state.edu (A.D. Kinghorn).



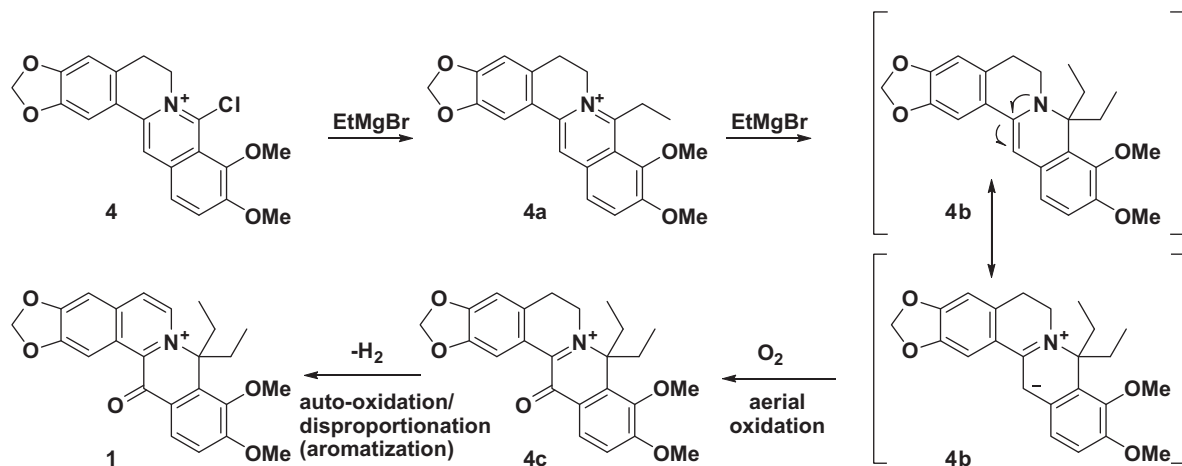
Scheme 1. Synthetic scheme for 5,6-didehydro-8,8-diethyl-13-oxodihydroberberine chloride (**1**).

the yield of this oxidized product can vary from run to run. A proposed mechanism from **1** to **4** is provided in [Scheme 2](#).

5,6-Didehydro-8,8-diethyl-13-oxodihydroberberine chloride (**1**) was isolated as yellow-orange needles, mp 159 °C. The HRESIMS yielded a molecular ion peak at m/z 406.1650 (calcd 406.1654 for $[M]^+$) corresponding to the elemental formula, $C_{24}H_{24}NO_5^+$. The UV spectrum showed absorption maxima at 212, 241, and 287 nm. On comparing the NMR spectra of compound **1** with those of berberine, no significant chemical shift changes were found for the methylenedioxy moiety on ring A or the methoxy groups on ring D. In addition to the absence of methylene protons (H-5 and H-6), and two aromatic proton signals similar to those found in the 1H NMR spectrum of berberine, the proton NMR spectrum of compound **1** exhibited two sets of ethyl group proton signals at δ_H 3.22 (2H, dd, $J = 15.4, 7.6$ Hz, H-1''), 2.71 (2H, dd, $J = 15.4, 7.4$ Hz, H-1') and 0.39 (6H, H-2' and H-2''), and two vicinal aromatic proton resonances at δ_H 8.60 and 9.23 (H-5 and H-6) with a coupling constant of 7.2 Hz. These variations suggested that ring B of berberine is aromatized and ring C substituted with two ethyl groups as a result of the Grignard reaction. In addition to those chemical shift differences corresponding to the aforementioned structural changes, a conjugated carbonyl carbon signal was found in the ^{13}C NMR spectrum of **1** at δ_C 177.1 and was assigned to C-13.

The determinations of the positions of the carbonyl group and the ethyl groups were supported by the analysis of correlations observed in 2D NMR experiments, including from the 1H - 1H COSY, HSQC, HMBC, and NOESY spectra. Correlations in the HMBC spectrum between the protons of the methyl and methylene units of the ethyl groups and C-8 at δ_C 79.7 suggested two ethyl groups are linked to the C-8 position. This assignment was further supported by the cross peaks present in the NOESY spectrum between the methyl group and methoxy protons at δ_H 4.04, as well as between the methylene protons and H-6 at δ_H 9.23. Correlations from H-12 at δ_H 8.27 to C-13 at δ_C 177.1 observed in the HMBC experiment indicated the carbonyl group to be located on ring C. Finally, the NMR carbon-carbon correlations network was determined by a ^{13}C - ^{13}C 2D INADEQUATE (Incredible Natural Abundance DoubleQUAntum Transfer Experiment)²⁶ spectrum, provided with the Supplementary data. Thus, the structure of compound **1** was determined as 5,6-didehydro-8,8-diethyl-13-oxodihydroberberine chloride. Selected key correlations observed in the 1H - 1H COSY, HMBC, and NOESY spectra are presented in [Figure 1](#).

A main challenge in the structure elucidation of 5,6-didehydro-8,8-diethyl-13-oxodihydroberberine chloride (**1**) was the lack of a strong carbonyl signal in the IR spectrum as might be expected



Scheme 2. Scheme depicting possible oxidative mechanisms at C-13 and between C-5 and C-6 for **4**.

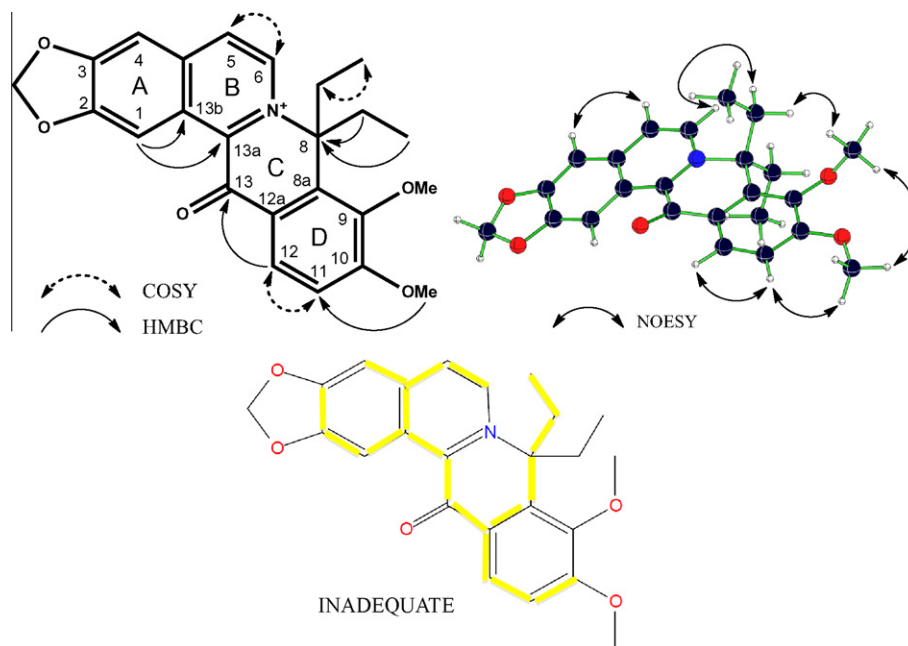


Figure 1. Key ^1H – ^1H COSY, HMBC, NOESY, and HMBC correlations for **1**.

in a structure of this type. Structural and spectroscopic properties of **1** were thus investigated computationally to obtain better insight regarding the missing carbonyl signal in the IR spectrum. For the study conducted, **1** was optimized at the DFT level using the meta-GGA hybrid M06 functional²⁷ and the 6-31+G** basis set. Solvation effects were taken into account using the IEFPCM solvation model²⁸ using the chloroform and methanol parameters as implemented in GAUSSIAN09.²⁹ Vibrational frequencies and intensities were then obtained by analytical computation at the same level. A scale factor of 0.950 on vibrational frequencies was used when comparing to experimental IR frequencies.

In the structural analysis, **1** presented a convex non-planar structure. Since the C-10 methoxy group points out of the plane of the compound, the existence of two non-equivalent conformations **1a** and **1b** are possible, which according to computed energies are nearly degenerate (Fig. 2).

On closer examination, it could be observed that only a signal of moderate intensity was observed in the IR spectrum of **1** at 1660 cm^{-1} . However, the computed vibrational IR spectrum elegantly predicted this lower intensity. Additionally, very good overall agreement was found between the computed and the experimental IR spectrum (Fig. 3).

As a further structural verification, chemical shifts were computed on M06/PCM(MeOH)/6-31+G** geometries using the DFT/

GIAO approach³⁰ with the meta-GGA non hybrid M06-L functional, which has proven recently to give accurate chemical shifts at moderate computational cost.³¹ We have employed the Jensen pcS-2 basis set, which has been specially designed for chemical shift DFT computations. Conformationally averaged isotropic chemical shielding constants were obtained as a linear average of computed shifts for forms **1a** and **1b** in a 50:50 ratio. Shieldings were then further averaged for all chemically equivalent nuclei. The isotropic chemical shielding constants were then converted into chemical shifts using Eq. (1).

$$\delta_{\text{calcd}} = -\sigma_{\text{calcd}} + \delta_{\text{ref}} \quad (1)$$

The offset δ_{ref} was obtained by least squares fitting the computed shifts to the experimentally observed ones. The quality of the fitting was expressed in terms of the root-mean-squared error RMSE and the maximum absolute error. For the ^1H prediction we obtained a RMSE of 0.31 and maximum absolute error of 0.72 ppm (Table 1), and for the ^{13}C prediction values were 2.87 and 9.30 ppm (Table 2), clearly showing the consistency of the studied structure with the experimental shifts.

Subsequently, the activity of 5,6-didehydro-8,8-diethyl-13-oxodihydroberberine chloride (**1**) was evaluated against several protozoan parasites using in vitro models of leishmaniasis, African trypanosomiasis, and malaria. The methods used for these assays

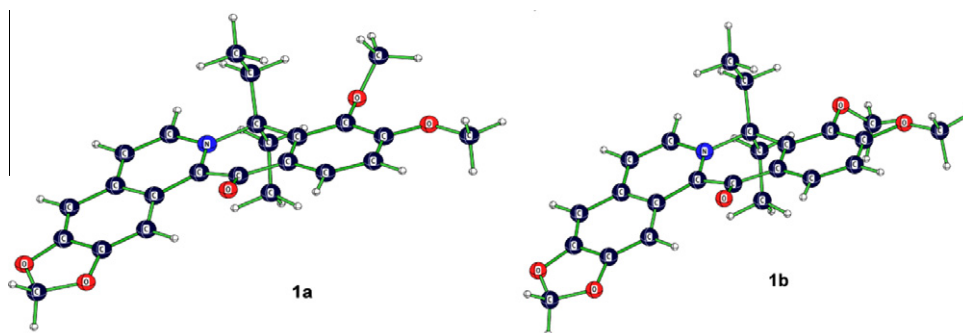


Figure 2. Optimized geometries for **1**.

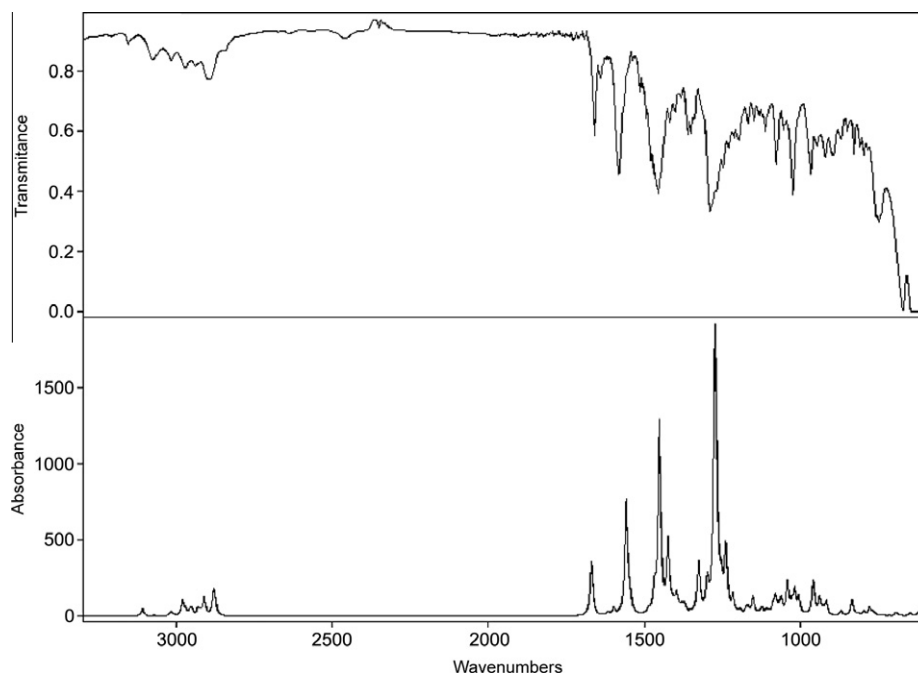


Figure 3. Top, experimental IR spectrum of **1** in CHCl_3 . Bottom, Computed M06/PCM(CHCl_3)/6-31+G** harmonic vibrational IR spectrum for species **1a** (Fig. 2). A scaling factor of 0.950 was applied to all frequencies. The spectrum was simulated using a line width of 10 cm^{-1} .

Table 1
Experimental (CD_3OD) and computed ^1H NMR chemical shifts for **1**

Nucleus	δ_{exp} (ppm)	δ_{calcd} (ppm)
H-1	9.09	9.13
H-4	7.68	7.50
H-5	8.61	8.31
H-6	9.22	8.51
H-11	7.54	7.44
H-12	8.26	8.48
CH-2a ^a	3.22	3.47
CH-2b ^b	2.70	2.44
CH_3	0.38	0.43
CH_3O (at C-10)	4.10	4.38
CH_3O (at C-9)	4.03	4.33
Methylenedioxy	6.45	6.88
RMSE (ppm)		0.31
MAE (ppm)		0.72

^a Shows NOE correlation with the methoxy group attached to C-9.

^b Shows NOE correlation with the H-6.

Table 2
Experimental (CD_3OD) and computed ^{13}C NMR chemical shifts for **1**

Nucleus	δ_{exp} (ppm)	δ_{calcd} (ppm)	Nucleus	δ_{exp} (ppm)	δ_{calcd} (ppm)
C-1	106.56	104.7	C-11	115.83	113.89
C-2	158.33	156.91	C-12	126.61	127.33
C-3	156.11	158.62	C-12a	124.70	120.97
C-4	104.39	102.54	C-13	178.50	176.24
C-4a	142.09	137.67	C-13a	142.37	139.49
C-5	129.31	127.67	C-13b	127.07	125.5
C-6	132.37	130.32	CH_2	35.14	38.21
C-8	81.11	85.28	CH_3	8.18	12.02
C-8a	133.30	133.98	CH_3O (C-10)	57.09	58.79
C-9	144.92	143.86	CH_3O (C-9)	61.67	63.8
C-10	160.85	161.27	C-11	115.83	113.89
RMSE (ppm)	2.87				
MAE (ppm)	9.30				

employing intracellular *Leishmania amazonensis*,³³ bloodstream form *Trypanosoma brucei brucei*,³⁴ and *Plasmodium falciparum*³⁵

have been reported previously. African green monkey kidney (Vero) cells were used as described earlier to determine the selectivity of **1** for parasites versus mammalian cells.³⁶ Following the in vitro assays, **1** was also studied in a murine model of visceral leishmaniasis described previously.³³ Summaries of the biological testing data on **1** are presented in Tables 3 and 4.

In the in vitro system for trypanosomiasis, **1** showed high inhibitory potency against *T.b. brucei* ($\text{IC}_{50} = 0.0091\text{ }\mu\text{M}$) and was more potent than the positive control drug, suramin. Antileishmanial activity was tested in murine peritoneal macrophages infected with *L. amazonensis* parasites. In this model, **1** exhibited an IC_{50} value of $0.18\text{ }\mu\text{M}$, a value comparable to amphotericin B, a clinically used drug employed as the positive control. In the case of *P. falciparum*, an assay employing flow cytometry was used and the IC_{50} value was determined to be $0.036\text{ }\mu\text{M}$, an activity comparable to chloroquine (Table 3). As can be inferred from these results, 8,8-diethyl substitution seems to result in a multiple-fold increase in all three bioassays when compared to the natural product, berberine.

In contrast, **1** did not exhibit cytotoxicity at the doses tested to Vero (green monkey epithelial kidney) cells, showing high selectivity towards parasites compared to mammalian cells. In the case of *T.b. brucei*, the selectivity was observed to be 10,000 (Table 3).

Considering the in vitro potency and selectivity of **1**, an efficacy study was performed in a mouse model of visceral leishmaniasis (Table 4). In this study, **1** caused a 47% reduction in liver parasitemia at a dose of $1\text{ mg/kg/day} \times 5$ administered ip. While this value indicated **1** might be more potent than miltefosine, which was tested at $10\text{ mg/kg/day} \times 5$, further in vivo studies indicated toxicity at doses higher than 1 mg/kg/day and the compound was not tested at higher doses. Despite this apparent limitation, the dialkyl substitution on C-8 of the berberine skeleton seems to increase antiprotozoal activity significantly and warrants further research on the structure–activity relationship of different substitutions at this position, along with mechanistic studies.

Table 3
Inhibitory activity (IC₅₀ values in μM)^a of 5,6-didehydro-8,8-diethyl-13-oxodihydroberberine chloride against *Trypanosoma brucei brucei*, *Leishmania amazonensis*, *Plasmodium falciparum*, and Vero cells

Sample name	<i>Trypanosoma brucei brucei</i>	<i>Leishmania amazonensis</i>	<i>Plasmodium falciparum</i>	Vero cell
Amphotericin B ^b	N/A	0.12 \pm 0.03	N/A	N/A
Chloroquine ^b	N/A	N/A	0.0087 \pm 0.0021	N/A
Suramin ^b	0.25 \pm 0.11	N/A	N/A	N/A
Berberine hemisulfate	1.1 \pm 0.1 ^c	17 \pm 5	0.80 \pm 0.31	N/A
5,6-Didehydro-8,8-diethyl-13-oxodihydroberberine chloride (1)	0.0091 \pm 0.0032	0.18 \pm 0.00	0.036 \pm 0.014	91 \pm 6

^a Mean \pm standard deviation unless otherwise noted ($n \geq 3$).

^b Positive controls.

^c Mean \pm range ($n = 2$).

Table 4
In vivo activity of 5,6-didehydro-8,8-diethyl-13-oxodihydroberberine chloride (1) in a mouse model for visceral leishmaniasis

Group	% Reduction in liver parasitemia (mean \pm standard deviation, $n = 4$)
5,6-Didehydro-8,8-diethyl-13-oxodihydroberberine chloride (1) ^a	47 \pm 4
Miltefosine ^b	98 \pm 1

^a 1 mg/kg/ip.

^b Positive control, 10 mg/kg/ip.

Acknowledgments

We kindly acknowledge Dr. James R. Fuchs, College of Pharmacy, The Ohio State University, for his valuable advice. We thank J. Fowle, College of Pharmacy, The Ohio State University, for facilitating the running of the NMR spectrometers. We also thank Dr. Kari Green-Church, Campus Chemical Instrument Center, The Ohio State University, for the mass spectrometry data. M.B. was supported by Jack L. Beal Graduate Student Award and Raymond W. Doskotch Fellowship, College of Pharmacy, The Ohio State University (2009–2010). Antileishmanial assays were funded by the Bill and Melinda Gates Foundation. NMR instrumentation used at Carnegie Mellon University was partially supported by NSF (CHE-0130903). ANV thanks Galician Consellería de Educación (2009/071) for financial support.

Supplementary data

Supplementary data associated with this article can be found, in the online version, at doi:10.1016/j.bmcl.2011.01.101.

References and notes

- Hotez, P. J.; Fenwick, A.; Savioli, L.; Molyneux, D. H. *Lancet* **2009**, 373, 1570.
- Liese, B.; Rosenberg, M.; Schratz, A. *Lancet* **2010**, 375, 67.
- Conteh, L.; Engels, T.; Molyneux, D. H. *Lancet* **2010**, 375, 239.
- Trouillier, P.; Oliaro, P.; Torreele, E.; Orbinski, J.; Laing, R.; Ford, N. *Lancet* **2002**, 359, 2188.
- Yamey, G.; Torreele, E. *Br. Med. J.* **2002**, 325, 176.
- Toreele, E.; Usdin, M.; Chirac, P. A. *Needs-based Pharmaceutical R&D Agenda for Neglected Diseases*; World Health Organization: Geneva, 2004.
- Hotez, P.; Ottesen, E.; Fenwick, A.; Molyneux, D. *Adv. Exp. Med. Biol.* **2006**, 582, 23.
- Hotez, P. J.; Molyneux, D. H.; Fenwick, A.; Kumaresan, J.; Sachs, S. E.; Sachs, J. D.; Savioli, L. *N. Eng. J. Med.* **2007**, 357, 1018.
- Neglected Tropical Diseases. <http://whqlibdoc.who.int/publications/> (accessed Aug 2010).
- Dewick, P. M. *Medicinal Natural Products: A Biosynthetic Approach*, 2nd ed.; John Wiley and Sons Ltd: Chichester, UK, 2002.
- Sinha, R.; Kumar, G. S. *J. Phys. Chem. B* **2009**, 113, 13410.
- Wang, Y. X.; Wang, Y. P.; Zhang, H.; Kong, W. J.; Li, Y. H.; Liu, F.; Gao, R. M.; Liu, T.; Jiang, J. D.; Song, D. Q. *Bioorg. Med. Chem. Lett.* **2009**, 19, 6004.
- Zhang, H.; Wei, J.; Xue, R.; Wu, J. D.; Zhao, W.; Wang, Z. Z.; Wang, S. K.; Zhou, Z. X.; Song, D. Q.; Wang, Y. M.; Pan, H. N.; Kong, W. J.; Jiang, J. D. *Metabolism* **2010**, 59, 285.
- Qi, M. Y.; Feng, Y.; Dai, D. Z.; Li, N.; Cheng, Y. S.; Dai, Y. *Acta Pharmacol. Sin.* **2010**, 31, 165.
- Iwazaki, R. S.; Endo, E. H.; Ueda-Nakamura, T.; Nakamura, C. V.; Garcia, L. B.; Filho, B. P. *Antonie van Leeuwenhoek* **2010**, 97, 201.
- Ghosh, A. K.; Bhattacharyya, F. K.; Ghosh, D. K. *Exp. Parasitol.* **1985**, 60, 404.
- Vennerstrom, J. L.; Klayman, D. L. *J. Med. Chem.* **1988**, 31, 1084.
- Vennerstrom, J. L.; Lovelace, J. K.; Waits, V. B.; Hanson, W. L.; Klayman, D. L. *Antimicrob. Agents Chemother.* **1990**, 34, 918.
- Nyasse, B.; Nkwengoua, E.; Sondengam, B.; Denier, C.; Willson, M. *Pharmazie* **2002**, 57, 358.
- Rosenkranz, V.; Wink, M. *Molecules* **2008**, 13, 2462.
- Saha, P.; Sen, R.; Hariharan, C.; Kumar, D.; Das, P.; Chatterjee, M. *Free Radical Res.* **2009**, 43, 1101.
- Nkwengoua, E. T.; Ngantchou, I.; Nyasse, B.; Denier, C.; Blonski, C.; Schneider, B. *Nat. Prod. Res.* **2009**, 23, 1144.
- (a) Moniot, J. L.; Kravetz, T. M.; Abd el Rahman, A. H.; Shamma, M. *J. Pharm. Sci.* **1979**, 68, 705; (b) 8-Oxoberberine was isolated as pale-yellow needle crystals and characterized spectroscopically: ¹H NMR (DMSO-*d*₆) δ 7.49 (1H, d, *J* = 8.7 Hz, H-11), 7.47 (1H, s, H-1), 7.39 (1H, d, *J* = 8.7 Hz, H-12), 7.07 (1H, s, H-13), 6.90 (1H, s, H-4), 6.07 (2H, s, OCH₂O-2), 4.11 (2H, t, *J* = 6 Hz, H-6), 3.87 (3H, s, -OCH₃, C-10), 3.77 (3H, s, -OCH₃, C-9), 2.86 (2H, t, *J* = 6 Hz, H-5); HRESIMS *m/z* 374.0978 [M+Na]⁺ (calcd. for [C₂₀H₁₇NO₅+Na]⁺, 374.1004); (c) 8-Chloroberberine chloride was isolated as an orange amorphous solid and characterized spectroscopically: ¹H NMR (CF₃COOD) δ 8.33 (1H, s, H-13), 7.99 (1H, s, H-11), 7.98 (1H, s, H-12), 7.34 (1H, s, H-1), 6.83 (1H, s, H-4), 6.02 (2H, s, OCH₂O-2), 5.09 (2H, t, *J* = 6.3 Hz, H-6), 4.12 (3H, s, -OCH₃, -9), 4.11 (3H, s, -OCH₃, -10), 3.18 (2H, t, *J* = 6.0 Hz, H-5); HRESIMS *m/z* 370.0863 [M+Na]⁺ (calcd. for [C₂₀H₁₇NO₅+Na]⁺, 370.0846); (d) 5,6-Didehydro-8,8-diethyl-13-oxodihydroberberine chloride was isolated as yellow needle crystals (MeOH/H₂O), mp 159 °C; UV (MeOH) λ_{max} (log ϵ) 212 (4.33), 241 (4.18), 287 (4.09) nm; IR (film) ν_{max} 3417, 1659, 1581, 1460, 1290, 1027 cm⁻¹; ¹H NMR (300 MHz, MeOD) δ 9.22 (1H, d, *J* = 7.2 Hz, H-6), 9.09 (1H, s, H-1), 8.61 (1H, d, *J* = 7.2 Hz, H-5), 8.26 (1H, d, *J* = 8.9 Hz, H-12), 7.68 (1H, s, H-4), 7.54 (1H, d, *J* = 8.9 Hz, H-11), 6.45 (2H, s, OCH₂O), 4.10 (3H, s, OCH₃/10), 4.03 (3H, s, OCH₃/9), 3.22 (2H, dd, *J* = 15.4, 7.6 Hz, H-1'), 2.70 (2H, dd, *J* = 15.4, 7.4 Hz, H-1'), 0.38 (6H, t, *J* = 7.4 Hz, H-2' and H-2''); ¹³C NMR (75 MHz, MeOD) δ 178.5 (C-13), 161 (C-10), 158.3 (C-2), 156.1 (C-3), 145.0 (C-9), 142.3 (C-13a), 142.0 (C-4a), 133.3 (C-8a), 132.3 (C-6), 129.3 (C-5), 127.0 (C-13b), 126.6 (C-12), 124.7 (C-12a), 115.8 (C-11), 106.6 (C-1), 106.3 (-OCH₂O-), 104.4 (C-4), 81.1 (C-8), 61.7 (OCH₃/9), 57.0 (OCH₃/10), 35.8 (C-1' and C-1''), 8.2 (C-2' and C-2''); HRESIMS *m/z* 406.1650 [M]⁺ (calcd. for C₂₄H₂₄NO₅, 406.1654); (e) Li, W.-D. Z.; Yang, H. *Tetrahedron* **2005**, 61, 5037.
- Iwasa, K.; Lee, D.-U.; Kang, S.-I.; Wiegreb, W. *J. Nat. Prod.* **1998**, 61, 1150.
- Cheng, Z.; Chen, A.-F.; Wu, F.; Sheng, L.; Zhang, H.-K.; Gu, M.; Li, Y.-Y.; Zhang, L.-N.; Hu, L.-H.; Li, J.-Y.; Li, J. *Bioorg. Med. Chem.* **2010**, 18, 5915.
- Bax, A.; Freeman, R.; Kempell, S. P. *J. Am. Chem. Soc.* **1980**, 102, 4849.
- Zhao, Y.; Truhlar, D. G. *Theor. Chem. Acc.* **2008**, 120, 215.
- Tomasi, J.; Mennucci, B.; Cammi, R. *Chem. Rev.* **2005**, 105, 2999.
- GAUSSIAN09, Rev. A.02: Frisch, M. J. et al. Gaussian, Wallingford, CT, 2004.
- Jensen, F. *J. Chem. Theor. Comput.* **2008**, 4, 719.
- Zhao, Y.; Truhlar, D. G. *J. Phys. Chem. A* **2008**, 112, 6794.
- Bifulco, G.; Dambruoso, P.; Gómez-Paloma, L.; Riccio, R. *Chem. Rev.* **2007**, 107, 3744.
- Delfin, D.; Morgan, R.; Zhu, X.; Werbovetz, K. *Bioorg. Med. Chem.* **2009**, 17, 820.
- Werbovetz, K.; Sackett, D.; Delfin, D.; Bhattacharya, G.; Salem, M.; Obrzut, T.; Rattendi, D.; Bacchi, C. *Mol. Pharmacol.* **2003**, 64, 1325.
- Liu, J.; Gluzman, I. Y.; Drew, M. E.; Goldberg, D. E. *J. Biol. Chem.* **2005**, 280, 1432.
- Salem, M.; Werbovetz, K. *J. Nat. Prod.* **2005**, 68, 108.